

# DETERMINATION OF BENTHIC OXYGEN CONCENTRATION UNDER THE KIELER MEERESFARM

This report has been funded by Bundesministerium für Bildung und Forschung Project No. 031B0915H2 AQUATOR “Akzelerator zur Entwicklung der aquatischen Bioökonomie” within the innovation cluster “Bioökonomie auf Marinen Standorten (BaMS).”

Project:	AQUATOR	Kontakt:
Presented by:	Dr. Ing. Dr. rer.nat Johan Vélez Franz Weinland Christian Lohaus Prof. Dr. Norbert Reintjes	Johan.velez@th-luebeck.de Franz.weinland@stud.th-luebeck.de christian.lohaus@th-luebeck.de norbert.reintjes@th-luebeck.de
Version:	Stand:	Changes
1.00	02.11.2021	First draft
2.00	23.11.2021	Adjustments from the THL team
3.00	26.11.2021	Adjustment from Peter Krost comments

## Table of Contents

Table of Contents .....	2
List of tables .....	3
List of figures .....	3
List of acronyms .....	4
Summary .....	5
Zusammenfassung.....	6
1 Introduction.....	7
2 Mussel production, benefits and burdens - a brief introduction. ....	7
2.1 Mussel farm and oxygen depletion.....	8
3 Description of the Kieler Meeresfarm.....	9
4 Material and methods .....	10
4.1 Temporal location of the data collection.....	11
4.2 Area definition.....	12
4.3 Measurement Procedure .....	14
4.3.1 First sampling event 13.09.2021.....	14
4.3.2 Second sampling event 08.10.2021 .....	15
5 Results.....	15
5.1 Results of the sampling event on 13.09.2021.....	15
5.1.1 Measuring conditions .....	15
5.1.2 Descriptive analysis .....	16
5.2 Results of the sampling event on 08.10.2021.....	17
5.2.1 Measuring conditions .....	17
5.2.2 Descriptive analyse.....	18
6 Discussion .....	19
7 Conclusions.....	21
A Appendix: Pictures of Materials used.....	23
B Appendix: Geo coordinates and measures at the sampling point .....	25
C Appendix: Selected images of the benthos at the KMF and the reference area .....	31
References.....	33

## List of tables

Table 1: Descriptive statistics at the bottom.....	16
Table 2: Test of homogeneity (above) and test of normality (bottom) of the samples.....	17
Table 3: Wilcoxon rank-sum test of the samples.....	17
Table 4: Descriptive statistics at the bottom and under 6 meter depth.....	18
Table 5: Test of homogeneity (above) and test of normality (bottom) of the samples.....	19
Table 6: Wilcoxon rank-sum test of the samples.....	19
Table 7: Geo-coordinates and measured parameters at the KMF on 13.09.2021.....	25
Table 8: Geo-coordinates and measured parameters at the reference area on 13.09.2021.....	26
Table 9: Geo-coordinates and measured parameters at the bottom of the KMF on 08.10.2021.....	27
Table 10: Geo-coordinates and measured parameters at 6 meters of depth of the KMF on 08.10.2021.....	28
Table 11: Geo-coordinates and measured parameters at the bottom of the reference area on 08.10.2021.....	29
Table 12: Geo-coordinates and measured parameters at 6 meters of depth of the reference area on 08.10.2021.....	30

## List of figures

Figure 1: Overview map KMF. QGis A coruna 3.10.11 / EPSG:3857.....	9
Figure 2: Satellite image KMF.(Coastal Resarch & Management (CRM), 2020).....	10
Figure 3: Measuring point arrangement of the double grid measurement defined for the samples at 13.09.2021. Elaborated by Franz Weinland. QGis 3.10.11-A coruna / EPSG:3857.....	13
Figure 4: Displacement of the reference measuring points. QGis 3.10.11-A coruna / EPSG:3857.....	14
Figure 5: Order of the sample taken. Yellow triangles (KMF), Green triangles (reference area), dark arrow (direction of sampling).....	15
Figure 6: Boxplot of the diferente variables measured at the KMF (Kieler Meeresfarm) and the reference at 13.09.2021.....	16
Figure 7: Boxplot of the different variables measured at the KMF (Kieler Meeresfarm) and the reference area at the bottom and at 6 meters of depth on 08.10.2021.....	18
Figure 8: Secchi- depth. Rope used in figure 11. ....	23
Figure 9: Go-pro camera.....	23
Figure 10: Pyramidal frame of welded aluminum. Foto provided by Leon Neuendorf.....	23
Figure 11: Rope.....	24
Figure 12: Multimeter WTW MultiLine® Multi 3630 IDS.....	24
Figure 13: Multimeter Hach HQ40d 2-channel in combination with an Intellical LDO10115 oxygen (Photo taken from <a href="https://www.fondriest.com/hach-intellical-ldo101-field-optical-do-sensors.htm">https://www.fondriest.com/hach-intellical-ldo101-field-optical-do-sensors.htm</a> ).....	24
Figure 14: Biodiversity at the bottom of the KMF. ID 22 (top left), ID 32 (top right), ID 43 (bottom left), ID 52 (bottom right). ....	31
Figure 15: Biodiversity at the bottom of the reference area. ID 13 (top left), ID 23 (top right), ID 24 (bottom left), ID 41 (bottom right). ....	32

## List of acronyms

cm	centimeter
DO	dissolved oxygen
KMF	Kieler Meeresfarm
LAWA	Bund-/Länderarbeitsgemeinschaft Wasser
m	meter
NE	north-east
OMC	organic matter content
SE	south-east
THL	Technische Hochschule Lübeck
TOC	total organic carbon
CRM	Coastal Research Management
NW	north-west
SW	south-west
GbR	Gesellschaft beschränkten Rechts
PSU	practical salinity unit
GmbH	Gesellschaft mit beschränkter Haftung
°C	degrees centigrade
s	second
mg	milligram
POM	particulate organic matter
GPS	global positioning system

## Summary

Mussel farming is increasing worldwide due to increasing demand for human consumption and also for their capability to provide multiple ecosystem services e.g. increase of water transparency and the promotion of macrophyte growth (Schröder et al., 2014), promote habitat to different species e.g. algae, worms, snails, crustaceans, and fish (Ysebaert et al., 2009) and eutrophication control (Lindahl et al., 2005; Nizzoli et al., 2005). The later has been catching the attention of government agencies and entrepreneurs given its potential to control eutrophication in degraded water bodies, such as the Baltic Sea (Lindahl et al., 2005; Lindahl & Kollberg, 2009; Petersen et al., 2014).

Nonetheless, the excretion of dissolved inorganic nutrients into the water column and the sedimentation of organic matter as faeces and pseudofaeces (commonly both jointly labelled as biodeposition) are discussed to potentially cause an ecosystem degradation under the farm and the vicinities, mainly due to an enrichment and redistribution of nutrients under the seabed (Christensen et al., 2003) and the depletion of dissolved oxygen (DO) that is needed to support benthic communities and benthic mineralization.

This document describes the methods and the results of a research that aimed to quantify and compare the oxygen content under the Kieler Meeresfarm (KMF), a mussel farm located in Kiel, Germany, and their vicinities. The goal of this research was to clarify whether there is any difference in the oxygen content of the farm and the vicinities at different depth profiles (bottom and at 6 meters).

The results show that the oxygen concentration measured over the course of both sampling events was above 4 mgL<sup>-1</sup>, staying far above hypoxic conditions (DO < 2 mgL<sup>-1</sup>). Additionally, images taken of the seafloor during sampling show evidence of the presence of higher-trophic organisms (sea stars, fish and mussels) (see Appendix C), indicative of non-hypoxic conditions.

According to the statistical analysis there is no evidence of differing median oxygen contents under the KMF and a reference site. Moreover, comparing the results with previous measures, the data suggest that the oxygen content has remained relatively constant across the year; however, such hypothesis must be proven and is highlighted as future research outlines.

## Zusammenfassung

Der weltweite Anstieg der Miesmuschelzucht ist zum einen auf den wachsenden Bedarf für den menschlichen Verzehr und zum anderen auf die Fähigkeit der Muscheln, vielfältige ökologische Leistungen zu erbringen, zurückzuführen. Dazu gehören unter anderem die Erhöhung der Wassertransparenz und das dadurch verbesserte Macrophytenwachstum (Schröder et al., 2014), die Aufwertung von Habitat durch Unterbrechung homogener Lebensräume und Nahrungseintrag für z.B. Algen, Würmer, Schnecken, Krustentiere und Fische (Ysebaert et al., 2009), und die Eindämmung von Eutrophierung (Lindahl et al., 2005; Nizzoli et al., 2005). Letzteres hat die Aufmerksamkeit von Regierungsbehörden und Unternehmern auf sich gezogen, da die Eutrophierungseindämmung in geschädigten Gewässern wie der Ostsee zunehmend an Bedeutung gewinnt (Lindahl et al., 2005; Lindahl & Kollberg, 2009; Petersen et al., 2014).

Nichtsdestotrotz gibt es Nachweise dafür, dass die Exkretion von gelösten anorganischen Nährstoffen in der Wassersäule und die Sedimentation von organischer Stoffen in Form von Fäkalien und Pseudofäkalien (beides wird gemeinhin als Biodeposition bezeichnet) zu Degradation von benthischen Lebensräumen führt (Forrest & Creese, 2006; Naylor et al., 2021; Ysebaert et al., 2009). Dies ist vor allem auf die Anreicherung und Umverteilung von Nährstoffen auf und im Meeresboden (Christensen et al., 2003) und die Abnahme des gelösten Sauerstoffs (DO) zurückzuführen, der ein Grundbedürfnis fast aller benthischen Lebensgemeinschaften darstellt und für Prozesse der benthischen Mineralisierung benötigt wird.

Das vorliegende Dokument beschreibt den Ansatz und die Ergebnisse der Forschungsarbeit zur Quantifizierung und zum Vergleich des Sauerstoffgehalts unter der Kieler Meeresfarm (KMF), einer Muschelzuchtanlage in Kiel, Deutschland, und einer Referenzfläche. Ziel des Projektes ist, festzustellen, ob die Sauerstoffgehalte am Meeresboden und auf 6m Tiefe an der KMF und der Referenzfläche systematische Unterschiede aufweisen.

Die Ergebnisse zeigen, dass der Sauerstoffgehalt an beiden Messtagen an allen Messpunkten über 4 mgL<sup>-1</sup> liegt. Hypoxische Verhältnisse (DO < 2 mgL<sup>-1</sup>) konnten nicht nachgewiesen werden. Fotos vom Benthos, die während der Messungen aufgenommen wurden, zeigten zudem eine hohe Abundanz von Makrofauna und -flora (Seesterne, Miesmuscheln und verschiedene Fischarten).

Statistische Analyse der Messwerte konnte keine signifikanten Unterschiede zwischen den Sauerstoffgehalten der KMF und der Referenzfläche nachweisen. Ein Vergleich mit älteren Messdaten lässt zudem vermuten, dass der Sauerstoffgehalt unter der KMF über das Jahr gesehen, relativ konstant ist. Weitere Messungen sind aber erforderlich, um diese Annahme weiter zu untersuchen.

## 1 Introduction

Under the umbrella of The Bioeconomy on Marine Locations BaMs (Bioökonomie auf Marinen Standorten) launched in 2019 and financed for 5 years with a budget of 20 million Euros by the Federal Ministry of Education and Research of the Germany, different projects were initiated with the main objective of endorsing and supporting the transition to a BLUE economy.

One of the projects launched by BaMs is the AQUATOR project (Akzelerator zur Entwicklung der aquatischen Bioökonomie) that, with the help of several competent partners such as AquaKultur Abtshagen GmbH, Carl von Ossietzky Universität Oldenburg – Zentrum für Umwelt- und Nachhaltigkeitsforschung, Christian-Albrechts-Universität zu Kiel, Botanik, Coastal Research & Management GbR, Gesellschaft für Marine Aquakultur mbH, Technische Hochschule Lübeck, Universitätsklinikum Schleswig-Holstein, Toxikologie aims to support sustainable development of individual bioeconomic activities in coastal aquatic and farming systems. In this regard the Technische Hochschule Lübeck (THL) carries out energy and material flow analysis as well as environmental modelling and evaluation. The THL further aims to identify parameters of relevance and include them in mentioned modelling procedures.

In this context, one of the reference systems currently under analysis by the AQUATOR project is the mussel farm KMF located in Kiel (Schleswig-Holstein). During the project it becomes clear, that oxygen-concentrations and the risk of oxygen-depletion is a topic of relevance for concerned stakeholders (authorities, operators, public).

To clarify the role of oxygen-depletion in open aquaculture, with focus on mussel/bivalve farms, an explorative literature review is conducted. Moreover, provide on-site data a measurement campaign is carried out to study oxygen-concentrations underneath the KMF and at a reference-site.

The present report first provides a brief introduction of the benefits and possible burdens of cultivated mussel production. Secondly, a short literature review associated with oxygen depletion caused by mussel farming is provided. Further, a description of the KMF as well as a presentation of some physico-chemical parameters of the farm are summarized. Furthermore, the material and methods used in this research are presented. Finally, the results are described and discussed.

## 2 Mussel production, benefits and burdens – a brief introduction.

Global aquaculture production has increased significantly in recent years from 26 million tonnes in 2000 to 46 million tonnes in 2018 (FAO, 2020). As part of this growth, mussel aquaculture production has increased 18,7% from 1,3 million tonnes to 2,5 million tonnes between 2000 and 2018 (FAO, 2020). Such increase may be attributed, among other economic factors such as the increased demand, to the fact that mussel farming is considered sustainable and environmentally-friendly compared with other aquaculture practices (Brigolin et al., 2009). Mussel farming can provide multiple ecosystems services e.g. eutrophication control (Lindahl et al., 2005; Nizzoli et al., 2005), increase of water transparency and the promotion of macrophyte growth (positive water quality indicators in the Water Framework Directive (WFD)) (Schröder et al., 2014), as well as promotion of habitat to different species e.g. algae, worms, snails, crustaceans, and fish (Ysebaert et al., 2009).

Mussels are filter-feeders and feed on the phytoplankton and organic matter present in the water column (Brigolin et al., 2009). Therefore, mussel cultivation does not require the use of feed that is responsible for about 56% of the

total impacts associated with Climate change in seafood production (Aubin et al., 2018; Bohnes et al., 2019). Additionally, mussels do not require the use of antibiotics (Iribarren et al. 2010b), that may potentially increase antimicrobial resistance, an issue that has been acknowledged as one of the biggest threats to global health and food security by the World Health Organization (WHO, 2020). Moreover, one ton of mussel has the potential to remove between 8,5 – 12 kg of nitrogen, between 0,6 – 0,8 kg of phosphorus and between 40 – 50 kg of carbon from the environment during harvesting (Gren et al., 2009; Lindahl & Kollberg, 2009) and it has been recognized as a prominent, cost-effective mechanism to remove nutrients from a water body compared with other abatement measures (Gren et al., 2009).

Therefore the production of mussel as an element of the EU Blue Growth strategy (European Commission, 2012) has been catching the attention of government agencies and entrepreneurs given its potential to control eutrophication in degraded water bodies, such as the Baltic Sea (Lindahl et al., 2005; Lindahl & Kollberg, 2009; Petersen et al., 2014). Thus, several projects such as the Baltic EcoMussel project (European Commission, 2013), the Baltic Blue Growth project (BBG) (European Commission, 2016), and the BONUS OPTIMUS project (European Commission, 2017) have been launched to quantify the possible benefit of farming mussels in the Baltic Sea.

Despite the above-mentioned environmental benefits of mussel farming, it is not exempt from potentially creating environmental burdens such as the excretion of dissolved inorganic nutrients into the water column, the sedimentation of organic matter as faeces and pseudofaeces (commonly both jointly labelled as biodeposition), the accumulation of dead or dislodged mussels on the bottom from farm structures above, depending of the physico-chemical conditions of the area, an enrichment and redistribution of nutrients under the seabed (Christensen et al., 2003) and the depletion of oxygen needed to support the benthic communities and the benthic mineralization. Thus, potentially contributing to the degradation of ecosystems.

## 2.1 Mussel farm and oxygen depletion

Oxygen fluxes to marine sediments are limited by its low solubility in seawater and its low diffusion rates into sediments (Nizzoli et al., 2005). Organic enrichment of sediments may temporally or permanently deplete the oxygen available in the area (Newell, 2004), commonly referred to as hypoxic ( $DO < 2 \text{ mg l}^{-1}$ ) or anoxic ( $DO < 0,5 \text{ mg l}^{-1}$ ) conditions. Anoxic conditions occur when dissolved oxygen supply is exceeded by the oxidation rate of organic matter in the sediment layer such as biodeposits. These conditions may result in the decoupling of nitrification-denitrification, the release of phosphate from sediment to the water column, an enhanced anaerobic metabolism and the formation of hydrogen sulfide ( $\text{H}_2\text{S}$ ) through sulfide reduction, a compound with toxic effects on large parts of the benthic infaunal community (Carlsson et al., 2012; Newell, 2004; Nizzoli et al., 2005).

As oxygen depletion depends mainly on two factors, the amount of organic matter present in a defined area (sedimentations, mainly due to biodeposition) and their associated dispersion; the water depth and current velocities play a crucial role in the rate of oxygen depletion. According to Nizzoli et al. (2005) oxygen depletion is expected to be lower in areas with temperate, deep waters with relatively high water flushing, whereas in shallow water depths with low tidal exchanges and high summer temperatures e.g. Mediterranean lagoons, the depletion may be significantly greater. Nizzoli et al. (2005) determined an oxygen consumption rate of  $264 \text{ mmol m}^{-2}\text{d}^{-1}$  under a mussel farm in the Sacca di Goro lagoon, Italy, a shallow eutrophic water body of 1,5m of depth without any mentionable water currents. In comparison, other studies at shellfish farms in more favourable hydrodynamic settings report much lower oxygen consumption rates e.g.  $62 \text{ mmol m}^{-2}\text{d}^{-1}$  for Tjärnö island-Sweden (water depth = 8-13 m, current velocity =  $3 \text{ cms}^{-1}$ ) (Dahlbäck & Gunnarsson, 1981),  $0,039 \text{ mmol m}^{-2}\text{d}^{-1}$  (water depth = 19 m, current velocity = 6-12  $\text{cms}^{-1}$ ) in New Zealand (Christensen et al., 2003), and  $164 \text{ mmol m}^{-2}\text{d}^{-1}$  (water depth = 8 m, current velocity not reported) in Denmark (Carlsson et al., 2009).

Regarding the Baltic sea, there was no study found with detailed information, however Kotta et al., (2020) suggest, from a monitoring of existing mussel farms report, that it doesn't have any negative effects on the local oxygen conditions at the sediment–water interface (Kotta et al., 2020).

### 3 Description of the Kieler Meeresfarm

The KMF is located on Holtenau's shore a district of Kiel, capital of Schleswig-Holstein, Germany (Figure 1). The farm started in 2010 as part of the Extractive Baltic Aquaculture of Mussels and Algae (EBAMA) project and is run by a private company Kieler Meeresfarm GmbH & Co. KG (Minnhagen, 2017) since 2014. The farm has a total area of 0,59 ha (104 x 57 m), and consists of nine submerged 80 m horizontal longlines, separated 7.5 m distance from each located in area that has between 7.5 and 11,5 m water deep and is delimited by yellow marker buoys relatively close to the shore (< 100 m) of the western shore of the Kiel Inner Fjord in front of the former site of the Naval Air Wing 5 (MFG-5) at 9luminiun 150 of the Baltic Sea (Figure 2)(Coastal Resarch & Management, 2020). Salinity in practical salinity units (PSU) at the farm site ranges from 2,6 to 22,4 PSU with a mean salinity of 14.3 PSU, a constant current velocity 1-3 cms<sup>-1</sup> from northeast to southwest, chlorophyll a (chl-a) values lower than 1.9 mgL<sup>-1</sup> , and an annual temperature range of 0 °C to 21 °C with an annual mean of 11 °C (Minnhagen, 2017; Schröder et al., 2014).



Figure 1: Overview map KMF. Qgis A corona 3.10.11 / EPSG:3857



Figure 2: Satellite image KMF.(Coastal Resarch & Management (CRM), 2020)

In 2018 the harvest of blue mussel yielded around 15 tonnes in mussel wet weight of which around 5 tonnes were of sufficient size for sale as fresh whole mussel (mussel length between 4,5 and 6 cm) (Coastal Resarch & Management, 2020). Sedimentation of organic biodeposition increased by 50% in January and 425% in March in comparison to a remote reference point 30 m from the farm (Peter Krost, pers. Comm) (Schröder et al., 2014) with sedimentation rates on the ranges of 5,68 and 11,49  $\text{gm}^{-2}\text{d}^{-1}$ . Organic carbon content of the sedimenting matter was determined to be 0,0371 kg C kg (sediment)<sup>-1</sup>. Sinking velocities are on the ranges of 0,66 and 0,84  $\text{cms}^{-1}$  with a mean of 0,73  $\text{cms}^{-1}$  (Süßle, 2018).

According to data from a thesis by Süßle (2018) the overall concentrations of dissolved oxygen over sample measurements (June to August 2018) is in the range of 9,85  $\text{mgL}^{-1}$  in 3 m of depth on June 15 and 3,96  $\text{mgL}^{-1}$  in a depth of 9 m on July 30. Moreover, findings regarding the depletion rates of oxygen suggest that it follows a linear decrease in a function of the amount of sediment (between -0,0156 and -0,0280  $\text{mg}(\text{O}_2) \text{L}^{-1}\text{min}^{-1}$ ). The specific depletion rates (SDR) of oxygen per gram of particulate organic matter (POM) estimated by the author is on average 0,0713  $\text{mg L}^{-1}\text{min}^{-1}\text{g}(\text{POM})^{-1}$ . Moreover, the model for oxygen depletion applied by Süßle, (2018) suggest a decrease of 11,52% of oxygen resulting in minimal oxygen concentration of 6,1839  $\text{mgL}^{-1}$ , an oxygen concentration far above the threshold for hypoxic conditions.

## 4 Materials and methods

To determine if there is a difference in oxygen-concentration between the mussel farm and a reference-site a statistical test was chosen.

Within KMF- and reference-area homogeneously distributed points were selected (see Figure 3). The statistical tests and data processing were performed using R Studio V4.1.1, an open-source software, used globally for statistical analysis.

At the first sampling date the oxygen measurements were conducted using a Hach HQ40d 2-channel multimeter in combination with an Intellical LDO10115 oxygen probe on 15m of cable. The electrodes were weighted using a brick tied to the stainless-steel body of the probe using rope. The measured depths were corrected by the distance from the probe's electrode heads to the bottom of the weight. This electrode also measures water temperature. On the first sample date, a salinity electrode of the type Intellical CDC40115 on 15m of cable was used until it failed halfway through the sampling process. No pH was measured on the first sampling day as no pH electrode with the required cable length was available.

At the second sampling date a sampling rig was used for measurements. The pyramidal frame of welded aluminum profiles has a basal area of 0,25 m<sup>2</sup> and has a side length of 50 cm at 45 cm of height. All sides of the pyramidal frame were open, so water can freely flow through it. Measured depths were corrected by the height of the sampling rig. Two divers lead weights were attached to two opposite upright edges of the pyramid. The electrodes were attached to the other two opposite upright edges of the frame pointing downward so that the electrode heads were approximately 25 cm above the bottom side of the pyramidal frame. The position was chosen to minimize the influence of dissolved oxygen consumption by sediment resuspension upon impact of the sampling rig. The open-bottom construction of the sampling rig helped minimize this effect. Oxygen and temperature measurements were conducted using the same multimeter as on the first sampling date. As no replacement for the damaged salinity probe was available, salinity measurements were omitted except for a singular salinity measurement at the beginning of sampling for salinity compensation of oxygen measurements with the Hach HQ40d multimeter. A second multimeter of the type WTW MultiLine® Multi 3630 IDS was used with a WTW IDS SenTix® 980 pH electrode and sufficient cable to measure pH across both sampling areas on the second sampling day (see A Appendix: Pictures of Materials used). Additionally, a GoPro Hero camera was mounted in a waterproof housing on the upper part of the pyramidal frame facing downwards to take photos of the seabed. The camera was programmed to take a photo every 5 seconds at all sample sites (see C Appendix: Selected images of the benthos at the KMF and the reference area for some selected images of the two areas).

In both sampling dates determination of the depth of the euphotic zone was done using a Secchi disc according to ISO 7027 (ISO, 2019). The line used for depth measurements was a braided polyethylene rope with 0,1 m increments. The rope was calibrated to the end of the carabine affixed to the bottom end of the rope.

The position of sampling sites, in both sampling dates, was determined using Google Earth on a global positioning system (GPS) capable smartphone. KML files were exported from Qgis containing the coordinates of the sample sites in decimal degrees and imported into a google earth project as KML-files. The location pins could then be located using the same project file on the smartphone with position feedback.

#### 4.1 Period of the data collection

The Harvest of blue mussels (*Mytilus edulis*) occurs at the KMF in the fall when the mussels have reached marketable size (Coastal Research & Management, 2020). As fresh mussels are difficult to keep for long periods and demand is stable over the fall season rather than a spike at the beginning of harvest season, mussel harvest is done continuously over the course of a few months, beginning in September. A total of 15 tons was produced in 2018 from which about one third of the mussels grow to sales size (4,5 – 6,0 cm), one third was up to 2 cm, large and were used for socking and another third, from > 2 cm to < 4 cm, was currently not usable and was dumped back into the

sea (CRM, 2020). The refusal of small mussels and losses during harvesting result in a large input of organic matter to the seafloor. Additionally, biodeposition of mussels is strongly correlated with mussel metabolic rates, stocking density, and availability of particulate organic matter (POM) in the water column (Larsen & Riisgård, 2016). Furthermore, sedimentation of organic matter unrelated to mussels is highest in September, October and November (Sverker & Kautsky, 1987). Combined, these factors result in maximum fluxes of organic material from the pelagic zone to the benthos, thus oxygen demand at the bottom can be assumed to be maximal during these months.

A total of two sampling events occurred. The first sampling event took place on 13.09.2021 and the second on 08.10.2021. For the second sampling date it was decided to measure twice at each sampling site, once at 6m of depth and once at the bottom in case that the depth profile of the new area selected doesn't matches with the KMF.

## 4.2 Area definition

To determine the minimal required distance between the mussel farm and the reference area scientific literature was reviewed. Hartstein & Stevens (2005) determined an impact radius of 30-50 m from the respective farm boundary in their study of particle distribution under and around three different mussel farms in New Zealand. Callier et al., (2006) determined a maximum radius of influence of 24.4 m for a farm in Canada. Similarly, Chamberlain (2002) and Giles & Pilditch (2004) indicated a maximum dispersal radius of 50 m or less for a farm in Scotland and new Zealand respectively. The flow velocities are 5-10  $\text{cms}^{-1}$  in Callier et al., (2006), 3.4-9.8  $\text{cms}^{-1}$  in Hartstein & Stevens (2005), 0.9-13  $\text{cms}^{-1}$  Chamberlain (2002) and 12.8  $\text{cms}^{-1}$  Giles & Pilditch (2004) and are thus comparable or greater than the mean flow velocity at the KMF of 1-3  $\text{cms}^{-1}$  (statement by Peter Krost). Moreover, Water depths cited range from 5-7 m in Callier et al., (2006), 11-15 m in Chamberlain (2002) and 8-42 m in Hartstein & Stevens (2005) and are thus comparable to or exceeding the depth at the KMF of 7.5 m to 11 m (Coastal Research & Management, 2020). A greater depth gives particles from faeces and pseudofaeces more sinking distance and thus extends the dispersal radius. Similarly, greater current velocities also increase the dispersal radius. As both current speed and water depth at the KMF are well within the range of conditions mentioned above, a minimum distance of 50 m from the reference point to the farm boundary seems sufficient. The initial placement of the reference area resulted in a minimum distance between KMF and reference area of around 100m. After readjusting the placement of the reference area, the minimal distance decreased to around 70m.

A total of 60 data points were chosen for the first sampling date (30 under the KMF and 30 under the reference area). Since it was decided for the second sampling date to measure two different depths at each sampling site, 6m and bottom, a total of 120 data points was gathered (60 under the KMF and 60 under the reference area).

For sampling at the mussel farm, the area was divided into a grid of 6 lines in a SW/NE orientation and 5 lines in SE/NW orientation. The grid lines in SW/NE orientation are called "horizontal" grid lines; grid lines in SE/NW orientation are called "vertical" grid lines. The side lengths of the KMF are 104 m in NE orientation and 57 m in SE direction. The intersections of the grid lines form the measurement points. The side lengths of the exclusion zone area resulted in a measuring point distance of 26 m in the NE direction and about 11 m in the SE direction. Sampling points were named by the matrix system with two figures, the first one being the line number, the second being the row number. Ahead of the matrix coordinate the prefix "KMF" was chosen for sampling points under the KMF.

The reference grid should be comparable in extension and orientation to the measuring grid. Minimum and maximum depth should also be comparable to the minimum and maximum depth of the measuring grid. The number of horizontal and vertical grid lines shall be identical to the measuring grid. The numbering shall be according to the same system as 6x5 matrix (Figure 3). The same assumptions and subdivisions apply to the spacing of the grid lines and consequently also to the measuring points of the reference grid as to the measuring grid over the KMF surface.

The reference grid was set to have similar side lengths and shape to cover a similar sized area. The same 6 by 5 grid was chosen. Minimum and maximum depth were also required to be comparable to the depths at the KMF. Naming of sampling points at the reference site was done in the same way, only with the prefix “REF” instead of “KMF”.



Figure 3: Measuring point arrangement of the double grid measurement defined for the samples at 13.09.2021.  
Elaborated by Franz Weinland. Qgis 3.10.11-A corona / EPSG:3857

After assessing and comparing the measured depths of the KMF and reference area (see results in section 5 Results) a repositioning of the reference grid by one measuring point distance in NW direction and one measuring point distance in SW direction was performed (Figure 4) to equalize sampling point depths in both areas. The shifting of the reference sampling points was performed in QGIS (see appendix B for the geoinformation of the different points selected for the campaign).

It is worth mentioning, that the KMF measures taken at the 13.09.2021 and the 08.10.2021 were conducted in the same area defined previously.



Figure 4: Adjustment of the reference measuring points. Qgis 3.10.11-A coruna / EPSG:3857

## 4.3 Measurement Procedure

### 4.3.1 First sampling event 13.09.2021

The coordinates of the targeted sampling point in the KMF and the reference farm were first stored in a GPS-capable smartphone. All the points were approached in a small inflatable boat with an outboard engine (property of CRM). Anchoring was neither necessary nor practical and measurements were taken as close as possible to the sampling point chosen given the weather conditions (wind and currents).

After launching the inflatable boat, the outer fastening buoy of the third shore-side longline was approached first. This mooring buoy is located on the KMF measuring point with the measuring point ID 32. After seizing the mooring line of the buoy, an attempt was made to determine current velocity with a mechanical hydrometric current meter of the type CF31 by OTT HydroMet. The current velocity at the KMF at the time of measurement was not sufficient to determine a value using the mechanical flow meter. The minimal current velocity measurable by the device is  $2,5\text{cm s}^{-1}$  (OTT HydroMet GmbH, 2021). No further attempt was made to determine flow velocity using the existing measuring device. Secchi depth was determined at the same sampling point (KMF measurement point 32). Since the measuring point had already been approached, the remaining parameters were then also determined at KMF sampling point 32.

To measure the remaining points, the measurement was started at KMF measuring point 11. A whole row was measured alternately in a north-easterly direction, followed by another row in a south-westerly direction, so that the measurement sequence followed a serpentine line. After completing the measurements under the KMF surface, the same measurement pattern was applied under reference surface. Starting at reference area measuring point 11, each measuring point was approached alternately in a north-easterly and south-westerly direction, row by row (see figure 5).

### 4.3.2 Second sampling event 08.10.2021

Like the first sampling event, sampling points were navigated to using the same GPS-capable smartphone in the same inflatable boat.

Secchi depth was determined at sampling point KMF-32 as done on the first sampling date. No further parameters were determined at this point. Sampling was started at sampling point 11 under the KMF and concluded in alternating lines of opposite direction (Figure 5). Once sampling under the KMF was finished, sampling under the reference area was started similarly to the KMF area at sampling point 11. Differently to the KMF area however, the second sampling line was started at sampling point 21 thereafter continuing the same alternating pattern as before.

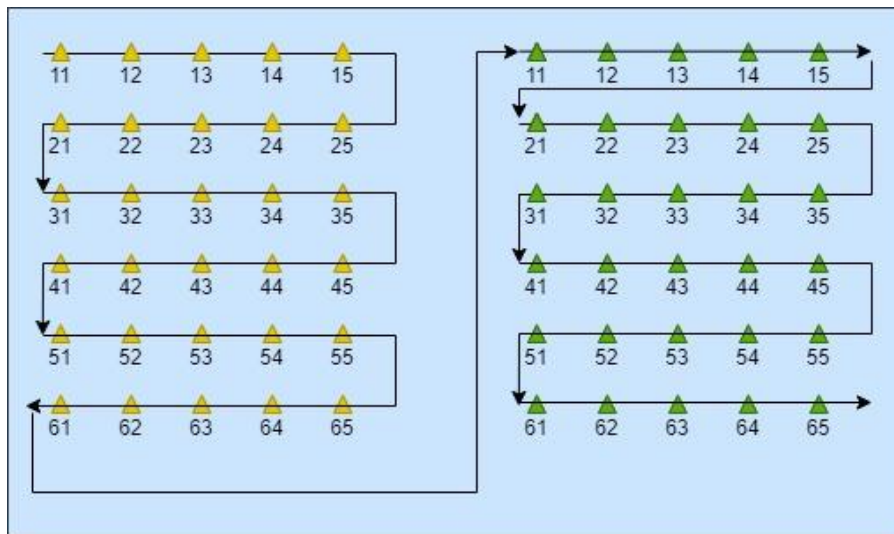


Figure 5. Order of the sample taken. Yellow triangles (KMF), Green triangles (reference area), dark arrow (direction of sampling)

At each sampling point the sampling rig was lowered to the bottom, indicated by a loosening of the rope and cable attached to the top of the sampling rig. Depth was determined on the tightened and vertical rope to the nearest 0,05m. After values stabilized, DO, temperature and pH (only on second sampling date) were recorded. Additionally, on the second sampling date a second set of parameters was determined at a depth of 6m. The rig was retrieved to Results.

## 5 Results

This section presents the results of the sampling events in chronological order. For each sampling date a description of the initial environmental conditions of the area on the selected day is given, followed by the statistical results.

### 5.1 Results of the sampling event on 13.09.2021

#### 5.1.1 Measuring conditions

The weather conditions that prevailed on the first day of measurement (13.09.2021) can be described as moderate. There was no precipitation during the measurement period. At the beginning of the measurements around 11 am, the wind was light to weak with 1-2 Beaufort from south-westerly direction. Towards the end of the measurement series at 2 pm, the wind increased to 3 Beaufort. The wind direction remained constant at SW. The outside temperature was 14°C to 17°C. The Secchi depth at the point 32 was determined at 8,00 m.

### 5.1.2 Descriptive analysis

The descriptive statistic (Table 1) shows that the all the variables different of temperature have a significant difference between the minimum and maximum value measured. Moreover, the boxplot (Figure 6) shows that variables measured are significantly more spreaded around the median for the reference area than the KMF.

Table 1: Descriptive statistics at the bottom of the two areas (KMF and reference)

Values at the KMF						
	Min	Max	Median	Mean	Std	Var
Tiefe (m)	7,1	13	10,79	10,46	1,7	2,9
Sauerstoff (mg/l)	7,2	9,43	8,61	8,55	0,64	0,41
Temperatur (°C)	17	17,9	17,7	17,59	0,23	0,05
Values at the reference area						
	Min	Max	Median	Mean	Std	Var
Tiefe (m)	8,65	13,5	12,4	12,05	1,16	1,35
Sauerstoff (mg/l)	3,5	9,12	7,3	6,76	1,64	2,71
Temperatur (°C)	16,6	17,8	17,25	17,13	0,37	0,14

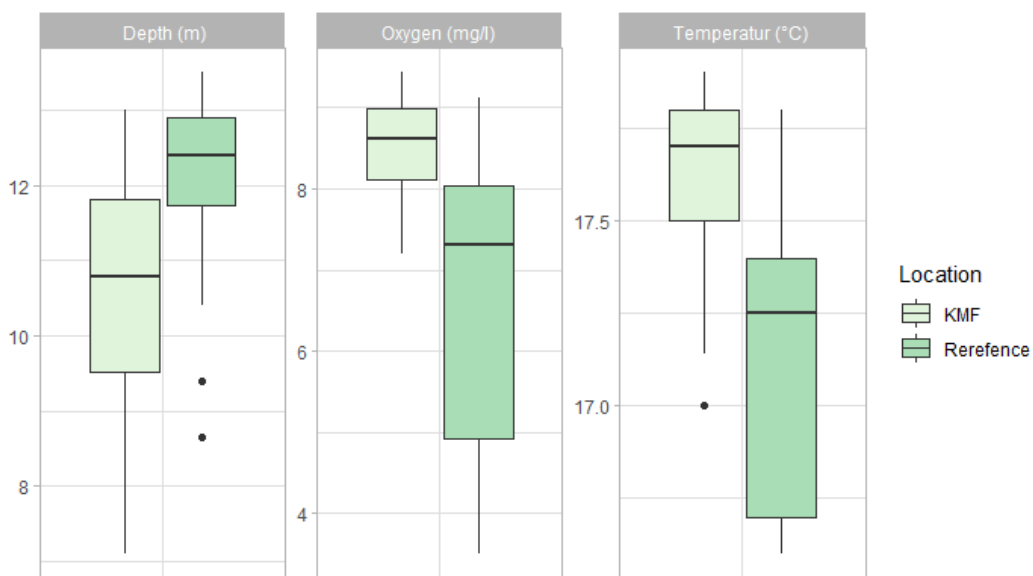


Figure 6: Boxplot of the different variables measured at the KMF (Kieler Meeresfarm) and the reference at 13.09.2021.

The Shapiro-Wilk test and the Levene test were chosen to check normality and homogeneity respectively in the samples (Table 2).

Table 2: Test of homogeneity (above) and test of normality (bottom) of the samples

Levene test (homogeneity)		
	Df	F-value
Bottom	1	14,256
		Pr(>F)
		0,0003***
Shapiro-Wilk test (normality)		
	w	P-value
Bottom	0,857	5,01E-06
Signif. codes: *** at 1%, ** at 5%, *at 10%		

The respective test results (Table 2) suggest that the variance of the samples are not equal (homoscedasticity) and are non-normally distributed. Therefore, the t-test (Pearson test) should not be applied as the results may be biased.

Therefore, to test if there is any significant difference in the median oxygen concentration between the KMF and the reference area the Wilcoxon rank-sum test (also known as Mann-Whitney-U-Test) is applied. The Wilcoxon rank-sum test is a non-parametric test for equal medians of two independent sample populations.

Table 3: Wilcoxon rank-sum test of the samples

Wilcoxon rank-sum test		
	w	P-value
Bottom	769	2,48E-06

According with the Wilcoxon test (see table 3) there is a statistical difference between the media of the samples, that is the median oxygen concentration at the bottom of the KMF are different to the median oxygen concentration under the reference farm.

## 5.2 Results of the sampling event on 08.10.2021

### 5.2.1 Measuring conditions

Overall conditions on the sampling day can be described as fair. There was no precipitation over the course of the sampling event. Upon arrival at the boat ramp, wind was light at 1 to 2 Beaufort. Shortly after sampling started at the farm site, low-hanging clouds and fog rolled in from SE, bringing with it winds of 3 to 4 Beaufort from the same direction. These conditions prevailed until sampling at the reference site started. Thereafter the clouds partly dispersed to a light cover with sunny periods. The wind calmed to 2 Beaufort with gusts at 3 Beaufort from NE.

Ambient temperatures ranged from 9 °C in the morning to 13 °C towards the end of the sampling event. The Secchi depth at the point 32 was determined at 3,60 m.

## 5.2.2 Descriptive analyse

Statistic analysis (Table 4 and Figure 7) shows that variables such as temperature and pH are relatively stable at the bottom and at 6 meters of depth in both areas (under the Reference and the mussel farm).

Table 4: Descriptive statistics at the bottom and under 6 meter depth for the two areas (KMF and reference) together

		Min	Max	Median	Mean	Std	Var
KML	Depth (m)	6,2	11,4	10,15	9,65	1,56	2,44
	Oxygen (mg/l)	4,36	7,65	6,16	6,18	0,99	0,99
	Temperature (°C)	14	15	14,85	14,81	0,18	0,03
	pH	7,57	7,92	7,81	7,78	0,09	0,01
Reference	Depth (m)	6	11,8	10,9	10,07	1,73	0,15
	Oxygen (mg/l)	4,33	8,37	5,52	5,94	1,79	3,02
	Temperature (°C)	14,7	15,3	15	14,97	0,11	1,39
	pH	7,6	8,12	7,69	7,77	0,15	0,01
Descriptive statistics at the 6 meter depth							
KML	Oxygen (mg/l)	7,08	8	7,75	7,68	0,25	0,06
	Temperature (°C)	14,7	14,8	14,7	14,74	0,04	0,002
	pH	7,84	8	7,94	7,92	0,03	0,001
Reference	Oxygen (mg/l)	6,29	8,49	7,88	7,76	0,66	0,44
	Temperature (°C)	14,7	15	14,85	14,86	0,08	0,007
	pH	7,77	8,02	8	7,94	0,08	0,007

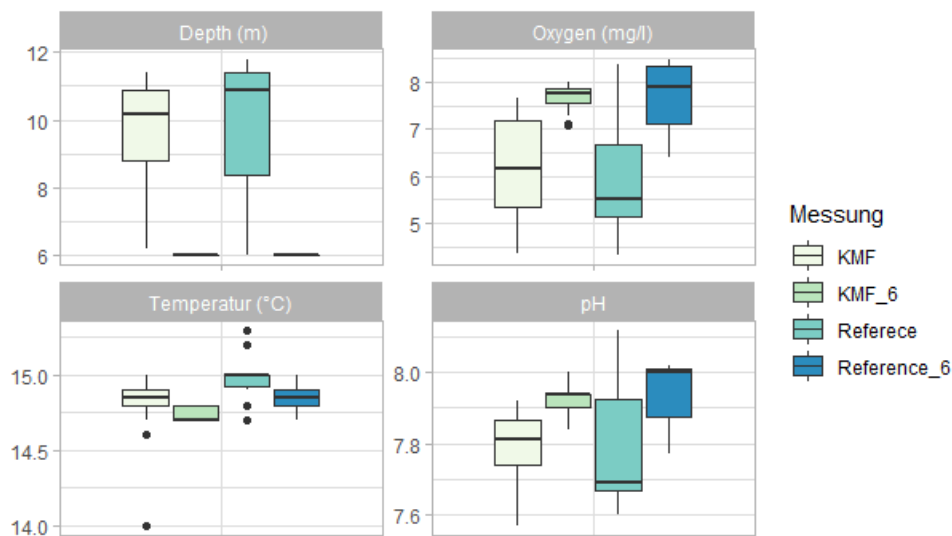


Figure 7: Boxplot of the different variables measured at the KMF (Kieler Meeresfarm) and the reference area at the bottom and at 6 meters of depth on 08.10.2021

The Shapiro-Wilk test and the Levene test were chosen to check normality and homogeneity respectively in the samples (Table 5: Test of homogeneity (above) and test of normality (bottom) of the samples).

Table 5: Test of homogeneity (above) and test of normality (bottom) of the samples

Levene test (homogeneity)			
	Df	F-value	Pr(>F)
Bottom	1	0,0506	0,8228
at 6 m depth	1	24,417	6,944E-6***
Shapiro-Wilk test (normality)			
	w	P-value	
Bottom	0,9488	0,01377	
at 6 m depth	0,9549	0,02675	

Signif. codes: \*\*\* at 1%, \*\* at 5%, \*at 10%

The respective tests (Table 2) show that both data sets are non-normally distributed. Therefore, the t-test (Pearson test) should not be applied to any of the samples as the results may be biased. Moreover, the Levene test shows that the median of the variance between the farm and the reference area are equal for the measurements at the bottom and non-equal for the parameters measured at 6 m depth.

Consequently, the Wilcoxon rank-sum test (also known as Mann-Whitney-U-Test) is applied to test if there is any significant difference in the median oxygen concentration between the farm and the reference area in both samples.

The results (Table 6) suggest that there is no significant difference between the median oxygen concentration between the farm and the reference area in any of the samples.

Table 6: Wilcoxon rank-sum test of the samples

Wilcoxon rank-sum test		
	w	P-value
Bottom	527,5	0,2549
at 6 m depth	374	0,2642

Signif. codes: \*\*\* at 1%, \*\* at 5%, \*at 10%

## 6 Discussion

For the first sampling date, results of the Wilcoxon rank-sum test suggest a difference between the oxygen medians for the two sample populations (KMF and reference area). This is mainly due to much higher variances of oxygen concentration under the reference area. Moreover, a deeper depth profile at the reference site compared to the KMF lead to lower oxygen concentrations at the reference site (Figure 6). Thus, the two sample sites cannot be compared and the results are considered biased by means of heterogeneity of depth of the two surveyed areas.

With the aim to ensure a comparable sampling, on 08.10.2021 a second sampling event took place. The position of the reference area was adjusted beforehand to account for the difference in depths under the survey areas, as described in Section 4.2. In addition to the relocation of the reference area, a second set of parameters was

measured at each sampling site at a depth of 6 m. The addition of a second data point for each sampling site was mainly introduced for time-cost reasons.

The rearrangement of the reference area was proven to be adequate (Figure 7). For the samples taken at the bottom, the depth profile of both areas was slightly slightly similar (between 6,20 and 11,40 m at the KMF and between 6 and 11,80 m at the reference area), although their corresponding variance were significantly different (2,44 at the KMF and 3,02 at the reference area). Consequently, the oxygen content boxplot (Figure 7) shows a greater spread for measurements taken under the reference compared with the KMF area. Moreover, the oxygen median of the two areas differ less than one-fold (6,16 mgL<sup>-1</sup> at the KMF and 5,52 mgL<sup>-1</sup> at the reference) and according to the Levene test (Table 5) the variances of the two samples are statistically similar (P- value = 0,82).

The oxygen measurements taken at 6 m of depth (Figure 7) show a considerable similarity as expected ( median value of 7,75 mgL<sup>-1</sup> for the KMF and 7,88 mgL<sup>-1</sup> for the reference area), although the oxygen values at the reference area are more spread than those obtained at the KMF where the values were quite constant (variance of 0,06 mgL<sup>-1</sup> at the KMF and 0,44 mgL<sup>-1</sup> at the reference area). In accordance with the Levene test (Table 5) the variances between the two areas are not similar. However, the medians of the two samples are quite similar.

Regarding oxygen concentrations at the KMF at 6 m of depth, two outliers were recorded at 7,08 mgL<sup>-1</sup> and 7,10 mgL<sup>-1</sup> at sampling sites KMF-12 and KMF-54 respectively. Given the fact that oxygen concentrations were not normally distributed (Table 5), neither at the bottom nor at 6m of depth, the Wilcoxon rank-sum test was conducted to test for equal medians of oxygen concentrations under the two sampled areas. The results suggest no statistical evidence of different oxygen concentrations at their respective depths.

Limitations regarding sampling efforts were mainly associated with weather conditions. Sampling dates were chosen primarily for their favourable wind forecasts, as high wind speeds can make sampling from boats very difficult. Despite the promising forecast, wind conditions changed suddenly around midday on 08.10.2021 and increased temporarily to a challenging 3-4 Beaufort. Moreover, stabilization time required by the multimeter was at times in conflict with the wind conditions, requiring slightly premature retrieval of the sampling rig at some sampling sites. Due to this conflict, some measured values may be slightly biased. However, as this conflict occurred across both sampling areas in no pattern, no significant influence on the results can be assumed.

Another important factor to be taken into account is the currents direction. In the surveyed area the current direction flows usually is from northeast to southwest (from the reference area to the KMF). It has, however, been observed that occasionally the current flow the other way around i.e. from southwest to northeast (from the KMF to the reference area). In such cases, the oxygen consumed below the mussel farm maybe pushes toward the reference station (Peter Krost, pers. Comm). The reference area would then be under the influence of the mussel farm and would thus no longer be a valid reference. Therefore, it is recommended to check the current direction ahead of sampling to ensure that such issues are avoided. Should the current direction be reversed ahead of sampling it should be considered to move the reference area upstream of the KMF as to avoid any influence on oxygen content. Additionally, it is not known if current reversals affect the oxygen content after the reversal event and if so, for how long. This uncertainty needs to be kept in mind. On both sampling days of this report however, current direction was from NE to SW with no visible reversal present at the time (personal observation).

No oxygen concentration measured over the course of both sampling events was lower than 4 mgL<sup>-1</sup> (between 4,36 and 9,43 mgL<sup>-1</sup> across the two measured areas), staying far above hypoxic conditions (DO < 2 mgL<sup>-1</sup>). Furthermore, images taken of the seafloor during sampling show evidence of the presence of higher-trophic organisms (sea stars, fish and mussels) (see C Appendix: Selected images of the benthos at the KMF and the reference area), indicative of non-hypoxic conditions.

The relatively high values of oxygen at the KMF may be attributed to different factors. Firstly, the size of the farm may be too small (less than 1 ha) to have any significant effect on the oxygen content at the bottom and their vicinities and secondly, as the KMF is located in an area with deep waters (between 7,5 m and 11,3 m) and moderate water flushing due to a mean current velocity between 3  $\text{cm s}^{-1}$  (Schröder et al., 2014). Nizzoli et al. (2005) suggest that in such areas the impacts of mussel farming on oxygen depletion are expected to be lower than those farms located in low water depth and currents.

Finally, comparing the results with those obtained by Süßle (2018) for oxygen samples taken between June and August at 9 m depth (6,1839  $\text{mg L}^{-1}$ ), the results presented are very similar to those obtained here in the same depth range under the KMF (between 6,27 and 7,27  $\text{mg L}^{-1}$ ) (List of figures B Appendix: Geo coordinates and measures at the sampling point). However, it is worth mentioning that the results provided by Süßle (2018) were calculated for locations well outside of the farm area.

Moreover, the model applied by Süßle (2018) was built upon several assumptions from which the results may be underestimated. Concretely, the initial oxygen concentration (9,85  $\text{mg L}^{-1}$ ) was obtained for a depth of 9 m and does not represent values close to the seafloor. Likely the oxygen concentration on the seafloor is lower. Furthermore, the dispersal of POM, for which the oxygen depletion model has been applied, was calculated with a relatively high current velocity (3,24  $\text{cm s}^{-1}$ ) compared with mean current velocity at the KMF (3  $\text{cm s}^{-1}$ ) (Schröder et al., 2014), resulting in higher dispersion and thus lower overall deposition. Higher deposition rates however go along with higher oxygen depletion and would shift conditions under the blue mussel farm closer to a state of hypoxia (Süßle, 2018).

Future research should aim to conduct a spatial-temporal analysis during harvesting to clarify whether the oxygen content under the KMF and the vicinities remain constant or for the contrary there are peaks of consumption at a particular time of the year. Moreover, given the fact that the median depth of the sampling areas is different (10,15 m and 10,90 m for the KMF and the reference area respectively) (see table 4) it is recommended not only to collect samples at 6 m depth, but also at different depth profiles i.e. at 9, 10, and 11 m depth to better test whether or not there is any significant impact of the mussel farming in the oxygen consumption of the area. Such results will provide scientific information that may help stakeholders to make future decisions regarding mussel farming. Moreover, such findings will help with the debate about the potential benefits and burdens of mussel farming.

## 7 Conclusions

This study measures and compares the oxygen content under the Kieler Meeresfarm and a reference area at different depths (bottom and at 6 m of depth). For doing so, a total of 120 parameter sets were measured on 08.10.2021 in both areas and processed in statistical software. The results suggest that there is no evidence of different oxygen concentrations in the two surveyed areas and the measuring period. Moreover, the evidence suggests that the oxygen concentrations under the farm (between 4,36 and 7,65  $\text{mg L}^{-1}$ ) and the vicinities (4,33 and 8,37  $\text{mg L}^{-1}$ ) are far from hypoxic conditions ( $\text{DO} < 2 \text{ mg L}^{-1}$ ).

Independent of the methodological differences between this study and the study conducted by Süßle (2018), a comparison suggest that the oxygen content under the KMF and the vicinities apparently remain relatively stable during the course of the years. However, a spatial-temporal during the course of the harvesting should be conducted to test such hypothesis.

To ensure more accurate measurements of the desired parameters it is recommended for future sampling events that winds do not to exceed 3 Beaufort. Sampling dates need to be picked in careful consideration of wind and

weather forecasts. Boat movements and drifting is practically unavoidable, however, careful selection of sampling dates based on forecasted weather conditions can greatly increase ease of sampling efforts.

## A Appendix: Pictures of Materials used



Figure 8. Secchi- depth. Rope used in figure 11.



Figure 9. Go-pro camera



Figure 10. Pyramidal frame of welded aluminium. Foto provided by Leon Neuendorf

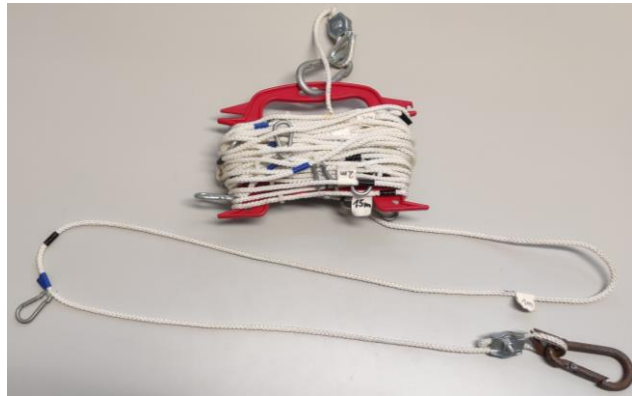


Figure 11. Rope



Figure 12. Multimeter WTW MultiLine® Multi 3630 IDS



Figure 13. Multimeter Hach HQ40d 2-channel in combination with an Intellical LDO10115 oxygen (Photo taken from <https://www.fondriest.com/hach-intellical-ldo101-field-optical-do-sensors.htm>)

**B Appendix: Geo coordinates and measures at the sampling point**

Table 7. Geo-coordinates and measured parameters at the KMF on 13.09.2021

Date	Measure	ID	Geo-coordinates		Parameter		
			X	Y	Depth	Oxygen	Temperature
13.09.2021	Meeresfarm	11	10,16214	54,37528	7,10	9,43	17,70
13.09.2021	Meeresfarm	12	10,16249	54,37550	7,30	9,39	17,80
13.09.2021	Meeresfarm	13	10,16282	54,37570	8,00	9,40	17,70
13.09.2021	Meeresfarm	14	10,16316	54,37592	7,80	9,14	17,80
13.09.2021	Meeresfarm	15	10,16350	54,37613	7,30	8,97	17,80
13.09.2021	Meeresfarm	21	10,16233	54,37515	10,25	8,75	17,60
13.09.2021	Meeresfarm	22	10,16268	54,37538	9,50	8,96	17,70
13.09.2021	Meeresfarm	23	10,16300	54,37560	10,15	8,64	17,70
13.09.2021	Meeresfarm	24	10,16335	54,37582	8,70	8,97	17,80
13.09.2021	Meeresfarm	25	10,16368	54,37604	9,55	9,40	17,80
13.09.2021	Meeresfarm	31	10,16253	54,37501	10,74	9,02	17,40
13.09.2021	Meeresfarm	32	10,16287	54,37526	11,00	8,45	17,60
13.09.2021	Meeresfarm	33	10,16319	54,37549	10,61	8,95	17,80
13.09.2021	Meeresfarm	34	10,16353	54,37572	10,47	8,44	17,70
13.09.2021	Meeresfarm	35	10,16386	54,37596	9,15	9,37	17,90
13.09.2021	Meeresfarm	41	10,16271	54,37489	11,34	8,85	17,80
13.09.2021	Meeresfarm	42	10,16306	54,37514	11,17	8,44	17,70
13.09.2021	Meeresfarm	43	10,16338	54,37537	10,55	8,99	17,80
13.09.2021	Meeresfarm	44	10,16372	54,37562	10,84	8,59	17,14
13.09.2021	Meeresfarm	45	10,16406	54,37586	11,14	8,37	17,70
13.09.2021	Meeresfarm	51	10,16292	54,37474	12,05	8,40	17,00
13.09.2021	Meeresfarm	52	10,16327	54,37501	11,79	8,00	17,50
13.09.2021	Meeresfarm	53	10,16359	54,37525	11,83	7,58	17,50
13.09.2021	Meeresfarm	54	10,16392	54,37551	10,90	7,90	17,50
13.09.2021	Meeresfarm	55	10,16425	54,37576	11,88	7,74	17,50
13.09.2021	Meeresfarm	61	10,16313	54,37460	12,20	7,20	17,30
13.09.2021	Meeresfarm	62	10,16347	54,37488	12,50	8,10	17,70
13.09.2021	Meeresfarm	63	10,16380	54,37514	12,50	8,14	17,30
13.09.2021	Meeresfarm	64	10,16411	54,37540	12,60	7,48	17,30
13.09.2021	Meeresfarm	65	10,16445	54,37567	13,00	7,53	17,20

Table 8. Geo-coordinates and measured parameters at the reference area on 13.09.2021

Date	Measure	ID	Geo-coordinates		Parameter		
			X	Y	Depth	Oxygen	Temperature
13.09.2021	Reference	11	10,16520	54,37663	8,65	9,12	17,80
13.09.2021	Reference	12	10,16561	54,37676	9,40	8,96	17,80
13.09.2021	Reference	13	10,16605	54,37691	10,70	8,72	17,60
13.09.2021	Reference	14	10,16644	54,37704	10,50	8,90	17,40
13.09.2021	Reference	15	10,16685	54,37717	11,70	8,30	17,50
13.09.2021	Reference	21	10,16536	54,37648	11,20	7,45	17,40
13.09.2021	Reference	22	10,16576	54,37662	10,40	8,10	17,50
13.09.2021	Reference	23	10,16622	54,37676	11,20	7,65	17,40
13.09.2021	Reference	24	10,16659	54,37689	12,10	7,60	17,40
13.09.2021	Reference	25	10,16697	54,37701	11,80	8,10	17,30
13.09.2021	Reference	31	10,16552	54,37632	11,90	7,53	17,30
13.09.2021	Reference	32	10,16593	54,37647	11,90	7,05	17,30
13.09.2021	Reference	33	10,16635	54,37661	12,20	7,20	17,30
13.09.2021	Reference	34	10,16672	54,37675	12,00	7,85	17,60
13.09.2021	Reference	35	10,16711	54,37687	12,30	7,48	17,40
13.09.2021	Reference	41	10,16565	54,37620	12,60	8,30	16,90
13.09.2021	Reference	42	10,16607	54,37633	12,70	6,50	16,90
13.09.2021	Reference	43	10,16651	54,37646	12,90	7,30	17,00
13.09.2021	Reference	44	10,16688	54,37661	12,60	7,30	17,00
13.09.2021	Reference	45	10,16726	54,37672	12,50	7,05	17,20
13.09.2021	Reference	51	10,16581	54,37605	12,90	5,30	16,80
13.09.2021	Reference	52	10,16621	54,37619	12,70	4,90	16,70
13.09.2021	Reference	53	10,16663	54,37633	12,80	4,80	16,70
13.09.2021	Reference	54	10,16703	54,37647	12,90	4,55	16,70
13.09.2021	Reference	55	10,16741	54,37660	13,10	3,50	16,70
13.09.2021	Reference	61	10,16597	54,37592	13,00	4,80	16,60
13.09.2021	Reference	62	10,16635	54,37607	13,50	4,50	16,70
13.09.2021	Reference	63	10,16678	54,37620	13,20	5,00	16,70
13.09.2021	Reference	64	10,16720	54,37633	13,15	4,84	16,70
13.09.2021	Reference	65	10,16754	54,37647	13,05	4,40	16,70

Table 9. Geo-coordinates and measured parameters at the bottom of the KMF on 08.10.2021

Date	Measure	ID	Geo-coordinates		Parameter			
			X	Y	Depth	Oxygen	Temperature	PH
08.10.2021	Meeresfarm	11	10,16214	54,37528	6,20	7,30	14,80	7,87
08.10.2021	Meeresfarm	12	10,16249	54,37550	6,30	7,37	14,70	7,86
08.10.2021	Meeresfarm	13	10,16282	54,37570	7,10	7,24	14,70	7,92
08.10.2021	Meeresfarm	14	10,16316	54,37592	6,80	7,65	14,60	7,92
08.10.2021	Meeresfarm	15	10,16350	54,37613	7,70	7,52	14,60	7,91
08.10.2021	Meeresfarm	21	10,16233	54,37515	8,50	6,75	14,80	7,83
08.10.2021	Meeresfarm	22	10,16268	54,37538	8,00	7,14	14,80	7,89
08.10.2021	Meeresfarm	23	10,16300	54,37560	9,40	7,19	14,90	7,82
08.10.2021	Meeresfarm	24	10,16335	54,37582	8,60	7,59	14,70	7,87
08.10.2021	Meeresfarm	25	10,16368	54,37604	9,50	6,75	14,80	7,89
08.10.2021	Meeresfarm	31	10,16253	54,37501	9,80	6,27	14,80	7,74
08.10.2021	Meeresfarm	32	10,16287	54,37526	9,80	6,50	14,80	7,82
08.10.2021	Meeresfarm	33	10,16319	54,37549	9,50	6,56	14,80	7,87
08.10.2021	Meeresfarm	34	10,16353	54,37572	9,50	7,27	14,80	7,86
08.10.2021	Meeresfarm	35	10,16386	54,37596	10,00	5,98	14,90	7,83
08.10.2021	Meeresfarm	41	10,16271	54,37489	10,30	6,05	14,90	7,80
08.10.2021	Meeresfarm	42	10,16306	54,37514	10,80	5,89	14,90	7,74
08.10.2021	Meeresfarm	43	10,16338	54,37537	10,40	6,27	14,90	7,72
08.10.2021	Meeresfarm	44	10,16372	54,37562	10,80	5,04	14,90	7,67
08.10.2021	Meeresfarm	45	10,16406	54,37586	10,55	4,70	14,90	7,63
08.10.2021	Meeresfarm	51	10,16292	54,37474	11,00	5,20	15,00	7,75
08.10.2021	Meeresfarm	52	10,16327	54,37501	11,00	5,79	14,80	7,76
08.10.2021	Meeresfarm	53	10,16359	54,37525	10,60	5,94	14,90	7,77
08.10.2021	Meeresfarm	54	10,16392	54,37551	10,30	5,53	14,90	7,72
08.10.2021	Meeresfarm	55	10,16425	54,37576	10,90	4,38	14,90	7,61
08.10.2021	Meeresfarm	61	10,16313	54,37460	11,20	5,82	14,90	7,82
08.10.2021	Meeresfarm	62	10,16347	54,37488	11,10	5,14	14,90	7,80
08.10.2021	Meeresfarm	63	10,16380	54,37514	11,30	5,27	14,00	7,75
08.10.2021	Meeresfarm	64	10,16411	54,37540	11,40	5,02	14,90	7,57
08.10.2021	Meeresfarm	65	10,16445	54,37567	11,30	4,36	15,00	7,65

Table 10. Geo-coordinates and measured parameters at 6 meters of depth of the KMF on 08.10.2021

Date	Measure	ID	Geo-coordinates		Parameter			
			X	Y	Depth	Oxygen	Temperature	PH
08.10.2021	Meeresfarm_6	11	10,16214	54,37528	6,00	7,30	14,80	7,87
08.10.2021	Meeresfarm_6	12	10,16249	54,37550	6,00	7,08	14,70	7,84
08.10.2021	Meeresfarm_6	13	10,16282	54,37570	6,00	7,96	14,70	7,97
08.10.2021	Meeresfarm_6	14	10,16316	54,37592	6,00	7,73	14,70	7,91
08.10.2021	Meeresfarm_6	15	10,16350	54,37613	6,00	7,66	14,70	7,91
08.10.2021	Meeresfarm_6	21	10,16233	54,37515	6,00	7,28	14,80	7,88
08.10.2021	Meeresfarm_6	22	10,16268	54,37538	6,00	7,58	14,70	7,89
08.10.2021	Meeresfarm_6	23	10,16300	54,37560	6,00	7,97	14,70	8,00
08.10.2021	Meeresfarm_6	24	10,16335	54,37582	6,00	7,94	14,70	7,87
08.10.2021	Meeresfarm_6	25	10,16368	54,37604	6,00	7,50	14,70	7,94
08.10.2021	Meeresfarm_6	31	10,16253	54,37501	6,00	7,82	14,70	7,94
08.10.2021	Meeresfarm_6	32	10,16287	54,37526	6,00	8,00	14,80	7,95
08.10.2021	Meeresfarm_6	33	10,16319	54,37549	6,00	7,55	14,80	7,94
08.10.2021	Meeresfarm_6	34	10,16353	54,37572	6,00	7,82	14,70	7,93
08.10.2021	Meeresfarm_6	35	10,16386	54,37596	6,00	7,74	14,80	7,94
08.10.2021	Meeresfarm_6	41	10,16271	54,37489	6,00	7,56	14,80	7,90
08.10.2021	Meeresfarm_6	42	10,16306	54,37514	6,00	7,95	14,80	7,94
08.10.2021	Meeresfarm_6	43	10,16338	54,37537	6,00	7,85	14,70	7,94
08.10.2021	Meeresfarm_6	44	10,16372	54,37562	6,00	7,75	14,70	7,93
08.10.2021	Meeresfarm_6	45	10,16406	54,37586	6,00	7,79	14,70	7,94
08.10.2021	Meeresfarm_6	51	10,16292	54,37474	6,00	7,84	14,80	7,94
08.10.2021	Meeresfarm_6	52	10,16327	54,37501	6,00	7,75	14,70	7,93
08.10.2021	Meeresfarm_6	53	10,16359	54,37525	6,00	7,65	14,70	7,94
08.10.2021	Meeresfarm_6	54	10,16392	54,37551	6,00	7,10	14,80	7,87
08.10.2021	Meeresfarm_6	55	10,16425	54,37576	6,00	7,35	14,80	7,89
08.10.2021	Meeresfarm_6	61	10,16313	54,37460	6,00	7,82	14,70	7,94
08.10.2021	Meeresfarm_6	62	10,16347	54,37488	6,00	7,45	14,80	7,90
08.10.2021	Meeresfarm_6	63	10,16380	54,37514	6,00	7,93	14,80	7,97
08.10.2021	Meeresfarm_6	64	10,16411	54,37540	6,00	7,83	14,70	7,94
08.10.2021	Meeresfarm_6	65	10,16445	54,37567	6,00	7,90	14,70	7,94

Table 11. Geo-coordinates and measured parameters at the bottom of the reference area on 08.10.2021

Date	Measure	ID	Geo-coordinates		Parameter			
			X	Y	Depth	Oxygen	Temperature	PH
08.10.2021	Reference	11	10,16464	54,37664	7,70	6,69	14,80	7,91
08.10.2021	Reference	12	10,16506	54,37678	8,25	7,25	14,80	7,85
08.10.2021	Reference	13	10,16550	54,37692	6,00	7,73	14,80	8,01
08.10.2021	Reference	14	10,16589	54,37705	7,10	8,27	14,80	8,01
08.10.2021	Reference	15	10,16629	54,37718	6,70	8,28	14,70	8,00
08.10.2021	Reference	21	10,16480	54,37649	8,30	6,68	15,20	7,93
08.10.2021	Reference	22	10,16520	54,37663	8,00	7,44	14,90	8,00
08.10.2021	Reference	23	10,16567	54,37677	8,00	8,37	14,80	7,99
08.10.2021	Reference	24	10,16604	54,37691	8,60	7,25	14,90	7,93
08.10.2021	Reference	25	10,16642	54,37702	10,10	4,94	15,00	7,67
08.10.2021	Reference	31	10,16496	54,37633	10,00	4,75	15,00	7,60
08.10.2021	Reference	32	10,16538	54,37648	10,30	4,81	15,00	7,60
08.10.2021	Reference	33	10,16580	54,37662	10,50	5,29	15,00	7,63
08.10.2021	Reference	34	10,16617	54,37677	10,75	5,29	15,00	7,63
08.10.2021	Reference	35	10,16656	54,37689	10,90	5,91	15,00	7,61
08.10.2021	Reference	41	10,10165	54,37621	10,90	4,33	15,00	7,70
08.10.2021	Reference	42	10,16552	54,37635	11,40	4,80	15,00	7,65
08.10.2021	Reference	43	10,16596	54,37647	11,40	5,36	15,00	7,66
08.10.2021	Reference	44	10,16633	54,37662	11,20	5,80	15,00	7,69
08.10.2021	Reference	45	10,16670	54,37673	11,30	5,69	15,00	7,72
08.10.2021	Reference	51	10,16525	54,37607	11,30	5,09	15,00	7,68
08.10.2021	Reference	52	10,16566	54,37620	11,30	5,00	15,00	7,67
08.10.2021	Reference	53	10,16607	54,37634	11,35	5,57	15,00	7,68
08.10.2021	Reference	54	10,16648	54,37648	11,40	5,39	15,00	7,67
08.10.2021	Reference	55	10,16685	54,37662	11,50	5,30	15,00	7,67
08.10.2021	Reference	61	10,16541	54,37593	11,40	4,70	15,30	7,68
08.10.2021	Reference	62	10,16580	54,37608	11,50	5,35	15,00	7,79
08.10.2021	Reference	63	10,16622	54,37621	11,55	5,55	15,00	7,73
08.10.2021	Reference	64	10,16664	54,37634	11,80	5,50	15,00	8,12
08.10.2021	Reference	65	10,16699	54,37648	11,60	5,93	15,00	7,69

Table 12. Geo-coordinates and measured parameters at 6 meters of depth of the reference area on 08.10.2021

Date	Measure	ID	Geo-coordinates		Parameter			
			X	Y	Depth	Oxygen	Temperature	PH
08.10.2021	Reference_6	11	10,16464	54,37664	6,00	7,83	14,70	7,97
08.10.2021	Reference_6	12	10,16506	54,37678	6,00	7,94	14,80	8,01
08.10.2021	Reference_6	13	10,16550	54,37692	6,00	7,73	14,80	8,01
08.10.2021	Reference_6	14	10,16589	54,37705	6,00	8,34	14,80	8,01
08.10.2021	Reference_6	15	10,16629	54,37718	6,00	7,58	14,80	8,00
08.10.2021	Reference_6	21	10,16480	54,37649	6,00	8,45	15,00	8,01
08.10.2021	Reference_6	22	10,16520	54,37663	6,00	8,49	14,80	8,02
08.10.2021	Reference_6	23	10,16567	54,37677	6,00	8,47	14,80	8,01
08.10.2021	Reference_6	24	10,16604	54,37691	6,00	8,40	14,80	8,01
08.10.2021	Reference_6	25	10,16642	54,37702	6,00	8,27	14,80	8,01
08.10.2021	Reference_6	31	10,16496	54,37633	6,00	8,46	14,80	8,02
08.10.2021	Reference_6	32	10,16538	54,37648	6,00	8,32	14,80	8,02
08.10.2021	Reference_6	33	10,16580	54,37662	6,00	8,39	14,80	8,01
08.10.2021	Reference_6	34	10,16617	54,37677	6,00	6,98	15,00	7,84
08.10.2021	Reference_6	35	10,16656	54,37689	6,00	6,94	15,00	7,77
08.10.2021	Reference_6	41	10,10165	54,37621	6,00	8,34	14,80	8,00
08.10.2021	Reference_6	42	10,16552	54,37635	6,00	8,27	14,80	8,00
08.10.2021	Reference_6	43	10,16596	54,37647	6,00	8,17	14,80	8,00
08.10.2021	Reference_6	44	10,16633	54,37662	6,00	7,83	14,90	7,94
08.10.2021	Reference_6	45	10,16670	54,37673	6,00	6,83	15,00	7,87
08.10.2021	Reference_6	51	10,16525	54,37607	6,00	8,40	14,90	8,02
08.10.2021	Reference_6	52	10,16566	54,37620	6,00	7,07	14,90	7,80
08.10.2021	Reference_6	53	10,16607	54,37634	6,00	7,01	14,90	7,84
08.10.2021	Reference_6	54	10,16648	54,37648	6,00	6,39	14,90	7,77
08.10.2021	Reference_6	55	10,16685	54,37662	6,00	6,39	15,00	7,78
08.10.2021	Reference_6	61	10,16541	54,37593	6,00	8,12	15,00	8,01
08.10.2021	Reference_6	62	10,16580	54,37608	6,00	7,48	14,90	7,90
08.10.2021	Reference_6	63	10,16622	54,37621	6,00	7,31	14,90	7,92
08.10.2021	Reference_6	64	10,16664	54,37634	6,00	7,55	14,90	7,89
08.10.2021	Reference_6	65	10,16699	54,37648	6,00	7,06	14,90	7,85

### C Appendix: Selected images of the benthos at the KMF and the reference area

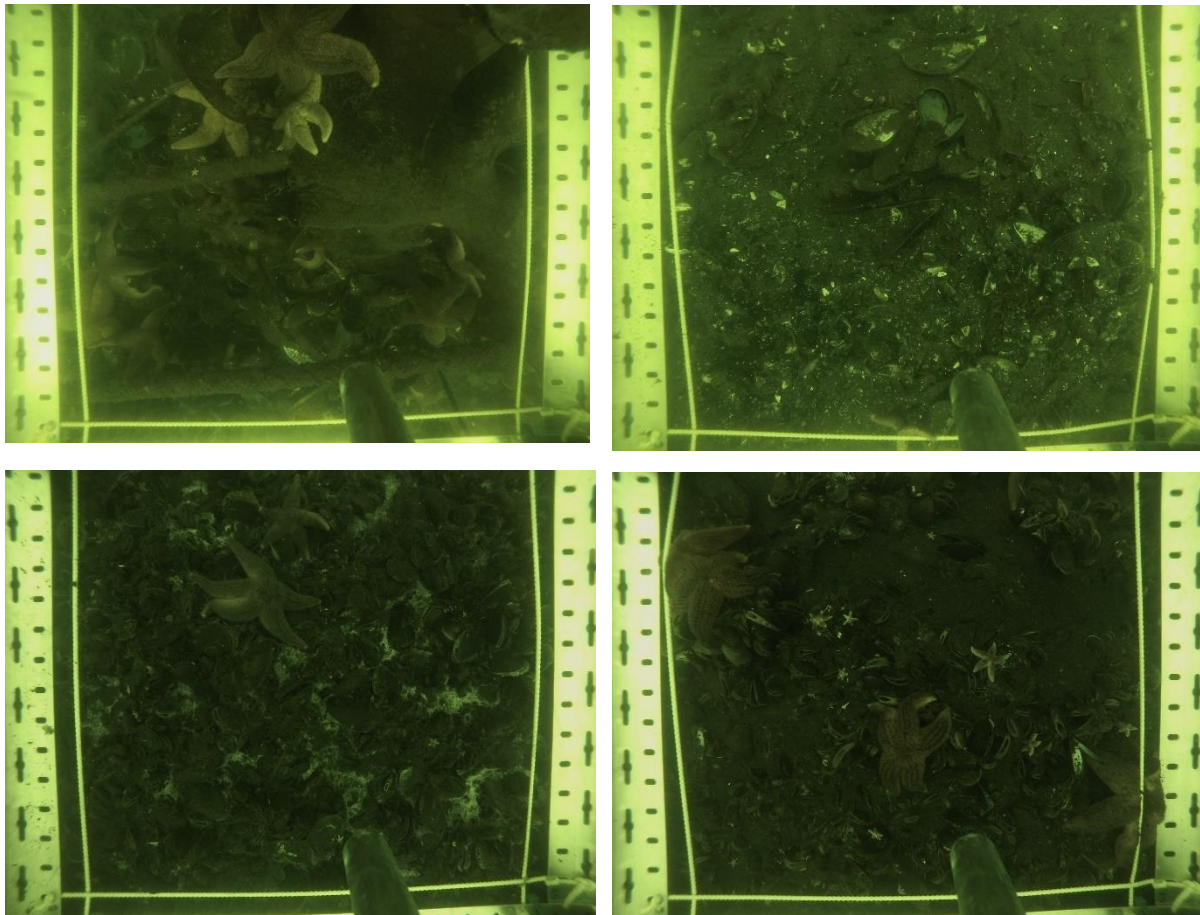


Figure 14. Biodiversity at the bottom of the KMF. ID 22 (top left), ID 32 (top right), ID 43 (bottom left), ID 52 (bottom right).

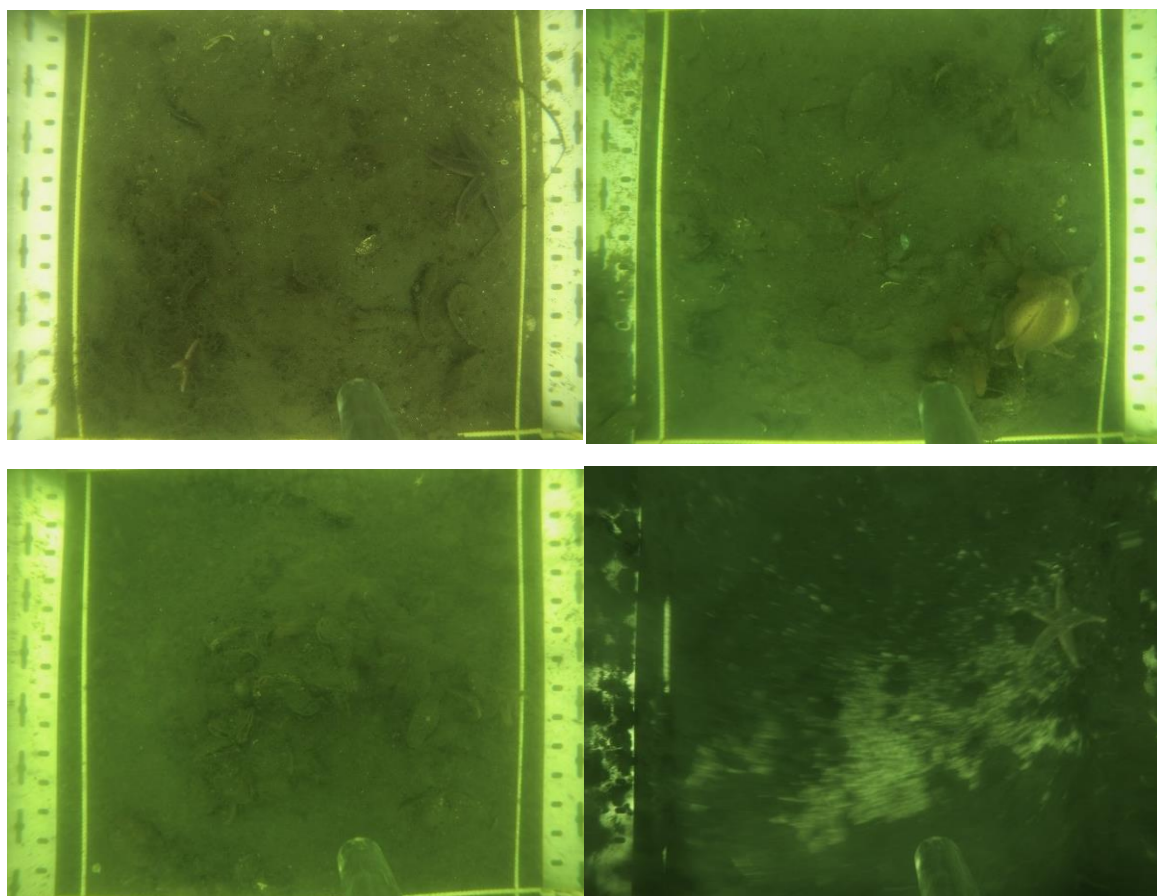


Figure 15. Biodiversity at the bottom of the reference area. ID 13 (top left), ID 23 (top right), ID 24 (bottom left), ID 41 (bottom right).

## References

- Aubin, J., Fontaine, C., Callier, M., & Roque d'orbcastel, E. (2018). Blue mussel (*Mytilus edulis*) bouchot culture in Mont-St Michel Bay: potential mitigation effects on climate change and eutrophication. *International Journal of Life Cycle Assessment*, 23(5), 1030–1041. <https://doi.org/10.1007/s11367-017-1403-y>
- Bohnes, F. A., Hauschild, M. Z., Schlundt, J., & Laurent, A. (2019). Life cycle assessments of aquaculture systems: a critical review of reported findings with recommendations for policy and system development. *Reviews in Aquaculture*, 11(4), 1061–1079. <https://doi.org/10.1111/raq.12280>
- Brigolin, D., Maschio, G. D., Rampazzo, F., Giani, M., & Pastres, R. (2009). An individual-based population dynamic model for estimating biomass yield and nutrient fluxes through an off-shore mussel (*Mytilus galloprovincialis*) farm. *Estuarine, Coastal and Shelf Science*, 82(3), 365–376. <https://doi.org/10.1016/j.ecss.2009.01.029>
- Callier, M. D., Weise, A. M., McKindsey, C. W., & Desrosiers, G. (2006). Sedimentation rates in a suspended mussel farm (Great-Entry Lagoon, Canada): Biodeposit production and dispersion. *Marine Ecology Progress Series*, 322(Hargrave 2005), 129–141. <https://doi.org/10.3354/meps322129>
- Carlsson, M. S., Engström, P., Lindahl, O., Ljungqvist, L., Petersen, J. K., Svanberg, L., & Holmer, M. (2012). Effects of mussel farms on the benthic nitrogen cycle on the swedish west Coast. *Aquaculture Environment Interactions*, 2(2), 177–191. <https://doi.org/10.3354/aei00039>
- Carlsson, M. S., Holmer, M., & Petersen, J. K. (2009). Seasonal and spatial variations of benthic impacts of mussel longline farming in a eutrophic danish fjord, limfjorden. *Journal of Shellfish Research*, 28(4), 791–801. <https://doi.org/10.2983/035.028.0408>
- Chamberlain, J. (2002). *Modelling the Environmental Impacts of Suspended Mussel (Mytilus edulis L.) Farming*. Napier University.
- Christensen, P. B., Glud, R. N., Dalsgaard, T., & Gillespie, P. (2003). Impacts of longline mussel farming on oxygen and nitrogen dynamics and biological communities of coastal sediments. *Aquaculture*, 218(1–4), 567–588. [https://doi.org/10.1016/S0044-8486\(02\)00587-2](https://doi.org/10.1016/S0044-8486(02)00587-2)
- Coastal Resarch & Management. (2020). *fact sheet Nr 1 Pilotsystem : Kieler Meeresfarm* (Issue 1).
- Coastal Resarch & Management (CRM). (2020). *fact sheet Nr 1 Pilotsystem : Kieler Meeresfarm* (Issue 1).
- Dahlbäck, B., & Gunnarsson, L. Å. H. (1981). Sedimentation and Sulfate Reduction Under a Mussel Culture. *Marine Biology*, 63(3), 269–275. <https://doi.org/10.1007/BF00395996>
- European Commission. (2012). Blue Growth – Opportunities for marine and maritime sustainable growth – Communication from the Commission to the european parliament, the Council, the european economic and social Committee and the Committee of the regions. In *Publications Office of the European Union*. <https://doi.org/10.2771/43949>
- European Commission. (2013). *Baltic EcoMussel project*. <http://projects.centralbaltic.eu/project/470-baltic-ecomussel>
- European Commission. (2016). *Baltic Blue Growth project*. <https://www.submariner-network.eu/balticbluegrowth>
- European Commission. (2017). *BONUS OPTIMUS project*. <https://www.bonus-optimus.eu/about>
- FAO. (2020). The State of World Fisheries and Aquaculture. Sustainability in action. In *Nature and Resources*. <https://doi.org/doi.org/10.4060/ca9229en>
- Giles, H., & Pilditch, C. A. (2004). Effects of diet on sinking rates and erosion thresholds of mussel Perna

- canaliculus biodeposits. *Marine Ecology Progress Series*, 282, 205–219.  
<https://doi.org/10.3354/meps282205>
- Gren, I. M., Lindahl, O., & Lindqvist, M. (2009). Values of mussel farming for combating eutrophication: An application to the Baltic Sea. *Ecological Engineering*, 35(5), 935–945.  
<https://doi.org/10.1016/j.ecoleng.2008.12.033>
- Hartstein, N. D., & Stevens, C. L. (2005). Deposition beneath long-line mussel farms. *Aquacultural Engineering*, 33(3), 192–213. <https://doi.org/10.1016/j.aquaeng.2005.01.002>
- Iribarren, D., Moreira, M. T., & Feijoo, G. (2010). Life Cycle Assessment of fresh and canned mussel processing and consumption in Galicia (NW Spain). *Resources, Conservation and Recycling*, 55(2), 106–117.  
<https://doi.org/10.1016/j.resconrec.2010.08.001>
- ISO. (2019). *EN ISO 7027: Water quality — Determination of turbidity — Part 2: Semi-quantitative methods for the assessment of transparency of waters* (p. 12). <https://www.iso.org/standard/69545.html>
- Kotta, J., Futter, M., Kaasik, A., Liversage, K., Rätsep, M., Barboza, F. R., Bergström, L., Bergström, P., Bobsien, I., Díaz, E., Herkül, K., Jonsson, P. R., Korpinen, S., Kraufvelin, P., Krost, P., Lindahl, O., Lindegarth, M., Lyngsgaard, M. M., Mühl, M., ... Virtanen, E. (2020). Cleaning up seas using blue growth initiatives: Mussel farming for eutrophication control in the Baltic Sea. *Science of the Total Environment*, 709.  
<https://doi.org/10.1016/j.scitotenv.2019.136144>
- Lindahl, O., Hart, R., Hernroth, B., Kollberg, S., Loo, L. O., Olrog, L., Rehnstam-Holm, A. S., Svensson, J., Svensson, S., & Syversen, U. (2005). Improving marine water quality by mussel farming: A profitable solution for Swedish society. *Ambio*, 34(2), 131–138. <https://doi.org/10.1579/0044-7447-34.2.131>
- Lindahl, O., & Kollberg, S. (2009). Can the EU agri-environmental aid program be extended into the coastal zone to combat eutrophication? *Hydrobiologia*, 629(1), 59–64. <https://doi.org/10.1007/s10750-009-9771-3>
- Minnhagen, S. (2017). Farming of blue mussels in the Baltic Sea: A review of pilot studies 2007-2016. *Baltic Blue Growth*.
- Newell, R. I. E. (2004). Ecosystem Influences of natural and cultivated Populations of suspension-feeding Bivalve Molluscs: A Review. In *Journal of Shellfish Research* (Vol. 23, Issue 1, pp. 51–61).
- Nizzoli, D., Welsh, D. T., Bartoli, M., & Viaroli, P. (2005). Impacts of mussel (*Mytilus galloprovincialis*) farming on oxygen consumption and nutrient recycling in a eutrophic coastal lagoon. *Hydrobiologia*, 550(1), 183–198.  
<https://doi.org/10.1007/s10750-005-4378-9>
- OTT HydroMet GmbH. (2021). *Technical Data OTT C31 Universal Current Meter for discharge measurements*. 1–2.
- Petersen, J. K., Hasler, B., Timmermann, K., Nielsen, P., Tørring, D. B., Larsen, M. M., & Holmer, M. (2014). Mussels as a tool for mitigation of nutrients in the marine environment. *Marine Pollution Bulletin*, 82(1–2), 137–143. <https://doi.org/10.1016/j.marpolbul.2014.03.006>
- Schröder, T., Stank, J., Schernewski, G., & Krost, P. (2014). The impact of a mussel farm on water transparency in the Kiel Fjord. *Ocean and Coastal Management*, 101(PA), 42–52.  
<https://doi.org/10.1016/j.ocecoaman.2014.04.034>
- Süßle, P. (2018). *Particulate Organic Matter Sedimentation and Ecological Consequences at a Blue Mussel Farm in the Kieler Förde*.
- Sverker, E., & Kautsky, N. (1987). Role of biodeposition by *Mytilus edulis* in the circulation of matter and nutrients in a Baltic coastal ecosystem. *Marine Ecology Progress Series*, 38(1952), 201–212.
- WHO. (2020). *Antibiotic resistance*. <https://www.who.int/en/news-room/fact-sheets/detail/antibiotic-resistance>

Ysebaert, T., Hart, M., & Herman, P. M. J. (2009). Impacts of bottom and suspended cultures of mussels *Mytilus* spp. on the surrounding sedimentary environment and macrobenthic biodiversity. *Helgoland Marine Research*, 63(1), 59–74. <https://doi.org/10.1007/s10152-008-0136-5>